Gaseous mercury flux from salt marshes is mediated by solar radiation and temperature

Article

Accepted Version

It is advisable to refer to the publisher's version if you intend to cite from the work. See Guidance on citing.

CentAUR

Central Archive at the University of Reading

Reading's research outputs online

1

Gaseous mercury flux from salt marshes is mediated by solar radiation and temperature

Tom Sizmur[1,2], Gordon McArthur[1,3], David Risk[3], Robert Tordon[4], and Nelson J. O'Driscoll[1]*

[1] Acadia University, Wolfville, Nova Scotia, Canada

[2] University of Reading, Reading, Berkshire, UK

[3] St. Francis Xavier University, Antigonish, Nova Scotia, Canada

[4] Environment Canada, Air Quality Branch, Dartmouth, Nova Scotia

*Department of Earth & Environmental Science, K.C. Irving Environmental Science Center, Acadia University, Wolfville, NS, B4P 2R6, Canada

10

Abstract

Salt marshes are ecologically sensitive ecosystems where mercury (Hg) methylation and biomagnification can occur. Understanding the mechanisms controlling gaseous Hg flux from salt marshes is important to predict the retention of Hg in coastal wetlands and project the impact of environmental change on the global Hg cycle. We monitored Hg flux from a remote salt marsh over 9 days which included three cloudless days and a 4 mm rainfall event. We observed a cyclical diel relationship between Hg flux and solar radiation. When measurements at the same irradiance intensity are considered, Hg flux was greater in the evening when the sediment was warm than in the morning when the sediment was cool. This is evidence to suggest that both solar radiation and sediment temperature directly influence the rate of Hg(II) photoreduction in salt marshes. Hg flux could be predicted from solar radiation and sediment temperature in sub-datasets collected during cloudless days ($R^2 = 0.99$), and before ($R^2 = 0.97$) and after ($R^2 = 0.95$) the rainfall event, but the combined dataset could not account for the lower Hg flux observed after the rainfall event that is in contrast to greater Hg flux from soils after rainfall events.

26

Introduction

Mercury (Hg) is a potent neurotoxin that accumulates at the top of aquatic food webs, often far away from emission sources due to long-distance atmospheric transport (Morel et al., 1998). The majority of Hg emitted into the atmosphere is gaseous elemental mercury, Hg(0), which has a residence time of several months in the atmosphere (Corbitt et al., 2011). Although recent efforts to phase out the use of Hg in commercial products has reduced atmospheric emissions (Zhang et al., 2016), anthropogenic sources currently account for only around 30% of emissions (UNEP, 2013). The remainder is attributed to natural sources (10%) and the re-emission of historically emitted anthropogenic sources (60%). The mechanisms underlying the emissions of Hg from ecosystems are imperfectly understood (Agnan et al., 2016). Improving our quantification of these fundamental processes is very important so that we can predict the impact that climate change will have on the global Hg cycle (Krabbenhoft and Sunderland, 2013), and the extent to which Hg will be retained in wetland environments where it can undergo methylation to methylmercury, which is more toxic and biomagnifies through the food web (Gregory Shriver et al., 2006).

Many of the previous attempts to quantify or mechanistically understand gaseous Hg flux from the terrestrial land surface have focussed on soils and freshwater wetlands (Agnan et al., 2016). Relatively little attention has been given to coastal wetlands. Although salt marshes do not represent a large portion of global surface area (they cover a global area of 3.8 x 10^7 Ha (Steudler and Peterson, 1984) which represents about 0.07% of the total land surface), they are an important Hg sink (Hung and Chmura, 2006). They provide conditions conducive to Hg methylation (Canário et al., 2007) and they support Hg-accumulating invertebrates at the base of sensitive food webs (Sizmur et al., 2013). Salt marshes may become more important sources of Hg flux in the future if more coastal wetlands are created by managed retreat responses to rising sea levels (Sizmur et al., 2016).

The mechanisms controlling Hg flux from coastal sediments is poorly understood since they have only been monitored during two studies (Sommar et al., 2013). Both studies found a positive relationship between Hg flux and solar radiation which indicates that emission of Hg(0) is due to photoreduction of Hg(II) and subsequent volatilisation (Lee et al., 2000; Smith and Reinfelder, 2009).

54   Lee et al (2000) also found a correlation between Hg flux and sediment temperature, but this

55   relationship is confounded due to the obvious correlation between temperature and solar radiation.

56   Moore and Carpi (2005) suggested that solar radiation mediates Hg(II) reduction to Hg(0) and that

57   temperature mediates the volatilisation of Hg(0) from soils. Pannu et al., (2014) identify a fast,

58   moisture-dependent abiotic process controlling reduction of a small Hg(II) pool, and a concurrent

59   slower biotic process that generates a larger pool of reducible Hg(II) in forest soils. Lindberg et al.

60   (2005; 2002) demonstrate that Hg(0) is volatilised during transpiration of wetland plants. The

61   applicability of these mechanistic insights have not been investigated in coastal wetlands.

62   There are some key differences between salt marshes and soils or terrestrial wetlands, such as the

63   influence of the tidal cycle, the considerably greater salinity and chloride concentration, and the

64   adaptations of salt marsh vegetation to the anoxic and saline environment. These differences may

65   result in different mechanisms that mediate Hg flux in coastal wetlands when compared to soils or

66   freshwater wetlands. We used a remote, non-point source mercury-contaminated salt marsh on the

67   Bay of Fundy, Nova Scotia, Canada as a model location to investigate Hg flux from coastal wetlands.

68

69   **Experimental**

70   Study site

71   The study took place between 6th and 15th July 2009. The study site was located at 45°9'13.61" N,

72   64°21'30.84"W in a salt marsh near the town of Kingsport on the shores of the Minas Basin of the

73   Bay of Fundy, Nova Scotia, Canada (Figure 1). The Bay of Fundy is well known for its high tidal

74   amplitude and large intertidal zone. The tide height can range >15 m in its upper reaches (Desplanque

75   and Mossman, 2001) with a typical period of 12.4 hours. Because of its proximity to the ocean and the

76   fact it sits close to sea level, the site periodically floods, but was not inundated during the study

77   period. Salt marsh cordgrass (*Spartina alterniflora*) is the dominant plant, while *Spartina pectinata*,

78   *Salicornia europaea*, *Cakile edentula* and *Spergularia marina* are also found in the area. The

79   sediment is a red-brown silty clay loam over strongly mottled brown-gray gleyed silty clay loam

80 derived from red-brown marine sediments. Air temperature during the study had a mean of 16.5°C

81 and reached as high as 27.1°C during the daytime and fell to a minimum of 7.5°C during the nights.

82 Wind speeds averaged 2.6 km hr^{-1} and gusted up to 20.9 km hr^{-1}.

83
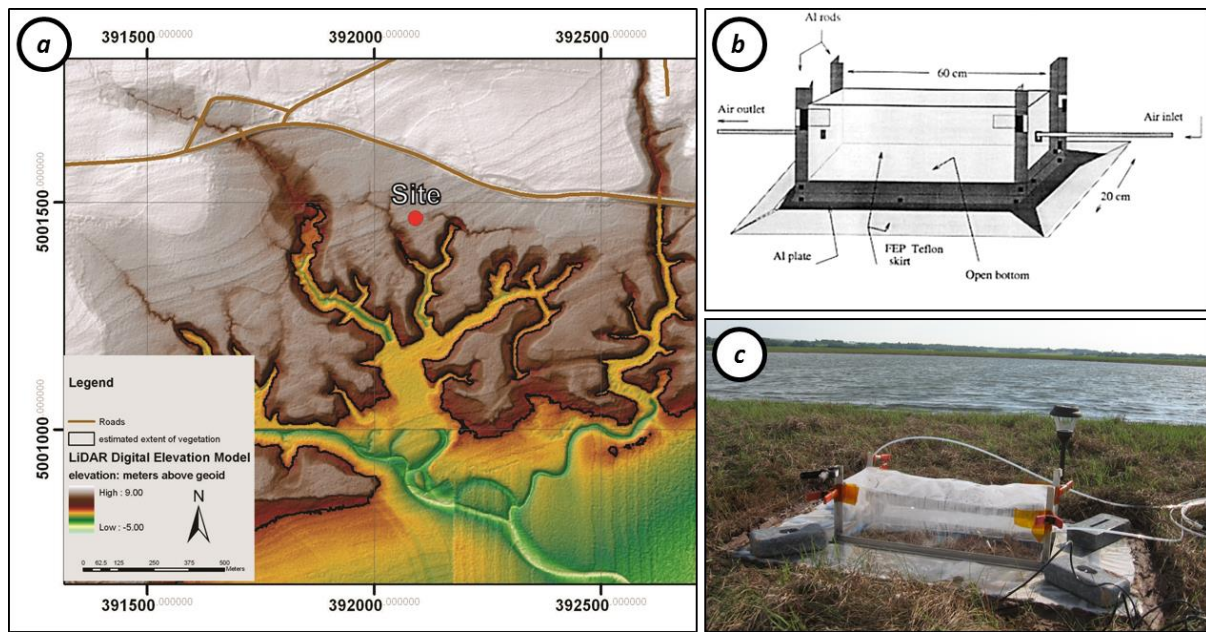
85 Figure 1 The location of the study site (a) identified on a digital elevation map of the salt marsh near
86 Kingsport, Nova Scotia, in the Minas Basin of the Bay of Fundy. Schematic (b) and photograph (c) of
87 the dynamic Hg flux chamber used to measure Hg flux at the site continuously over a 9-day period.

88

89 <u>Sediment sampling and total mercury analysis</u>

90 Two 30 cm sediment cores were sampled at the site using a polypropylene hand corer and transported

91 to the lab for sectioning. Core sections were separated into mineral and vegetation components in

92 >18.2 MΩ water and dried for 72 hours in a drying oven at 40°C. Dried samples were homogenized

93 with a mortar and pestle and all equipment was cleaned between samples using water and trace grade

94 ethanol. Vegetation samples were flash frozen with liquid nitrogen to aid in the homogenization

95 process. Wet and dry mass of samples were recorded and total mercury in samples was determined by

96 thermal degradation of samples and gold amalgamation atomic absorbance analysis using a Nippon

97 MA-2000.

98

Dynamic Hg Flux Chamber Technique

Gaseous Hg flux was measured every 10 minutes over the 9-day study period from 6th to 15th July 2009 using a dynamic flux chamber technique based on the method described by Carpi and Lindberg (Carpi and Lindberg, 1997). A Durafilm© chamber (20 cm H x 20 cm W x 60 cm L), covering an area 0.12 m^2 and made of 5 mil Teflon, was set on the sediment surface (Figure 1). Through an inlet and outlet at either end of the chamber ambient air was pumped through the chamber at a constant rate of 1.5 dm^3 min^{-1}, following Agnan et al.(2016). Dead air periods in the chamber were avoided by using a Tekran switching controller and second pump with a mass flow controller.

Mercury concentration at the inlet of the chamber reports the ambient concentration, while the mercury concentration at the outlet reports the chamber concentration. The inlet and outlet Hg concentrations were measured and compared using a dual channel Tekran Model 2537 mercury analyzer and used to calculate Hg flux (ng m^{-2} h^{-1}) from the dynamic chamber using the equation:

$$\text{Hg flux} = \frac{[\text{Hg}]o - [\text{Hg}]i}{A} \times Q$$

Where [Hg]o is the Hg concentration (ng m^{-3}) of air measured at the outlet, [Hg]i is the Hg concentration (ng m^{-3}) at the inlet, A denotes the area (0.12 m^2) of the bottom of the chamber in contact with the system measured and Q is the flow rate (1.5 dm^3 min^{-1}) of air through the chamber.

The dual channel Tekran analyser sampled two successive 5 minute air samples from the chamber inlet, followed by two successive 5 minute air samples flowing from the chamber outlet, ensuring that both gold cartridges were used for measuring both inlet and outlet air and any degradation of trap recoveries could be easily identified. Subsequently the flux was measured every 10 minutes. The time required to completely recycle the air in the chamber was about 16 minutes.

Prior to deploying the chamber at the study site the chamber system was tested for recovery of Hg(0) using standard injections from a Tekran 2505 mercury vapour external calibration unit and a Hamilton digital syringe. Recovery rates of Hg(0) injected into the chamber were consistently >90%.

123 Recoveries were also tested via manual injections in the field every 48 hours with similar recoveries

124 (>90%). As such data were not recovery corrected. Chamber blanks were also measured over a clean

125 Teflon sheet using mercury free air. The level of mercury measured in the mercury-free gas and

126 chamber air was below the detection limit of 0.01ng m^{-3}. Field measurements less than 0.01 ng m^{-3}

127 were treated as nondetectable (0 readings) in the dataset.

128

129 <u>Meteorological Sensors</u>

130 A Davis weather station recorded relative humidity, air temperature, wind speed, solar radiation and

131 barometric pressure at the study site. In addition, Campbell Scientific 107b thermistors were installed

132 to measure temperature of (i) the sediment 4 cm underneath the flux chamber, (ii) the air inside the

133 flux chamber, and (iii) the air outside the chamber every 5 minutes and coupled to a Campbell

134 Scientific CR1000 datalogger.

135 The intensity and spectral distribution of incoming solar radiation was quantified using an

136 OceanOptics USB 4000 spectroradiometer with a fibre-optic (10 m length, 200 um diameter) and

137 spectral diffusion probe (diameter 4.3 mm). The spectroradiometer probe was fastened to the outside

138 of the frame supporting the mercury flux chamber approximately 20 cm above the ground surface.

139 Based on controlled measurements in the lab, there is <12% loss of UV radiation (280-400 nm)

140 through the flux chamber Teflon film. Spectral readings were taken continuously every 5 minutes

141 during the field campaign for UVA (280-320 nm), UVB (320-400 nm), visible (400-800 nm), and

142 total UV-visible radiation (280-800 nm) and integrated using spectra suite software.

143 Because meteorological measurements were taken every 5 minutes and Hg flux only calculated every

144 10 minutes, Hg flux measurements were matched to the average of two sequentially collected

145 meteorological measurements.

146

147

148 **Results and discussion**

149 Concentration of total Hg in the sediments

150 The concentration of total Hg in the sediments ranged between 1.6 and 22.1 ng g^{-1} in the top 35 cm of

151 the mineral sediments (Figure 2), peaking at a depth of 12 cm. Concentrations in the root biomass

152 were considerably higher, ranging between 39.0 and 223.4 ng g^{-1} and showing a similar depth profile

153 to the mineral sediment (Figure 1). Sediment Hg concentrations (Figure 1) were within the range of

154 previous wetland and mudflat observations in the Minas Basin of the Bay of Fundy (O'Driscoll et al.,

155 2011; Sizmur et al., 2013) but considerably lower than salt marsh sites affected by local point-source

156 pollution (Canário et al., 2010; Mitchell and Gilmour, 2008).
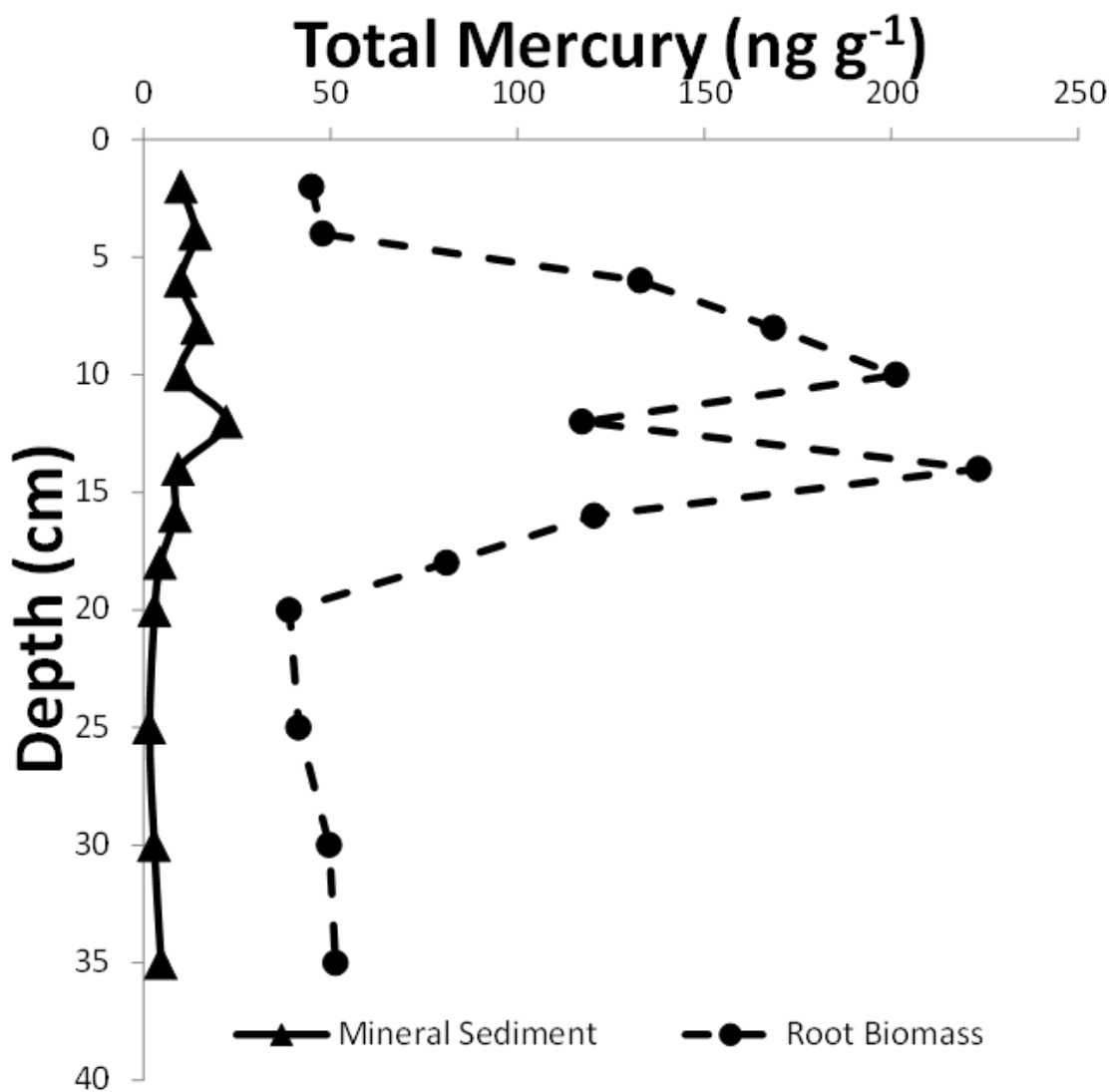
158 Figure 2 Total mercury concentration with depth in mineral sediments and root biomass at the site.

159 Gaseous Hg flux measurements from salt marshes

160   The Hg flux ranged -0.61 to 4.83 ng m^{-2} hr^{-1} during the course of the 9-day monitoring period with an

161   overall mean of 1.17 ng m^{-2} hr^{-1} (Figure 3). These fluxes are an order of magnitude lower than those

162   observed from the Great Bay estuary (mean 17 ng m^{-2} hr^{-1}), a non-point source mercury-contaminated

163   (450 ng g^{-1}) salt marsh in New Jersey (Smith and Reinfelder, 2009). The negative values we observed

164   (18.4% of total observations) occurred during the night time and are thought to have been due to Hg

165   deposition. In contrast, Lee et al. (2000) observed negative flux during the daytime and an overall

166   negative flux (mean -3.3 ng m^{-2} hr^{-1}) at a non-point source mercury-contaminated (200-470 ng g^{-1}) salt

167   marsh in Connecticut during a similar period of the year (Day 180-200 in 1998). Both studies

168   described above were conducted at sites that, despite being non-point source mercury-contaminated,

169   had sediment Hg concentrations (450 ng g^{-1} and 200-470 ng g^{-1}) more than an order of magnitude

170   greater than our site (1.6-22 ng g^{-1}; Figure 2). Both studies also used the micrometeorological method

171   to measure Hg flux (Sommar et al., 2013).

172   Our study used the dynamic flux chamber method to monitor Hg flux from a salt marsh. The

173   temperature in the dynamic flux chamber is usually greater than the ambient air temperature and so

174   often results in the measurement of artificially higher fluxes than the micrometeorological method

175   (Agnan et al., 2016) but can exhibit lower concentrations due to the absence of turbulence (Zhu et al.,

176   2015b). Zhu et al (2015b) found that dynamic flux chamber measurements lagged 2 hours behind Hg

177   flux measured using the micrometeorological methods and exhibited a positive bias in the afternoon

178   due to the changes in soil temperature lagging behind air temperature (Zhu et al., 2015a). However,

179   the dynamic flux chamber offers a greater capability to link the environmental conditions in and under

180   the specific chamber area to the Hg flux observed (especially in heterogeneous environments or in

181   coastal zones where wind direction changes diurnally).

182
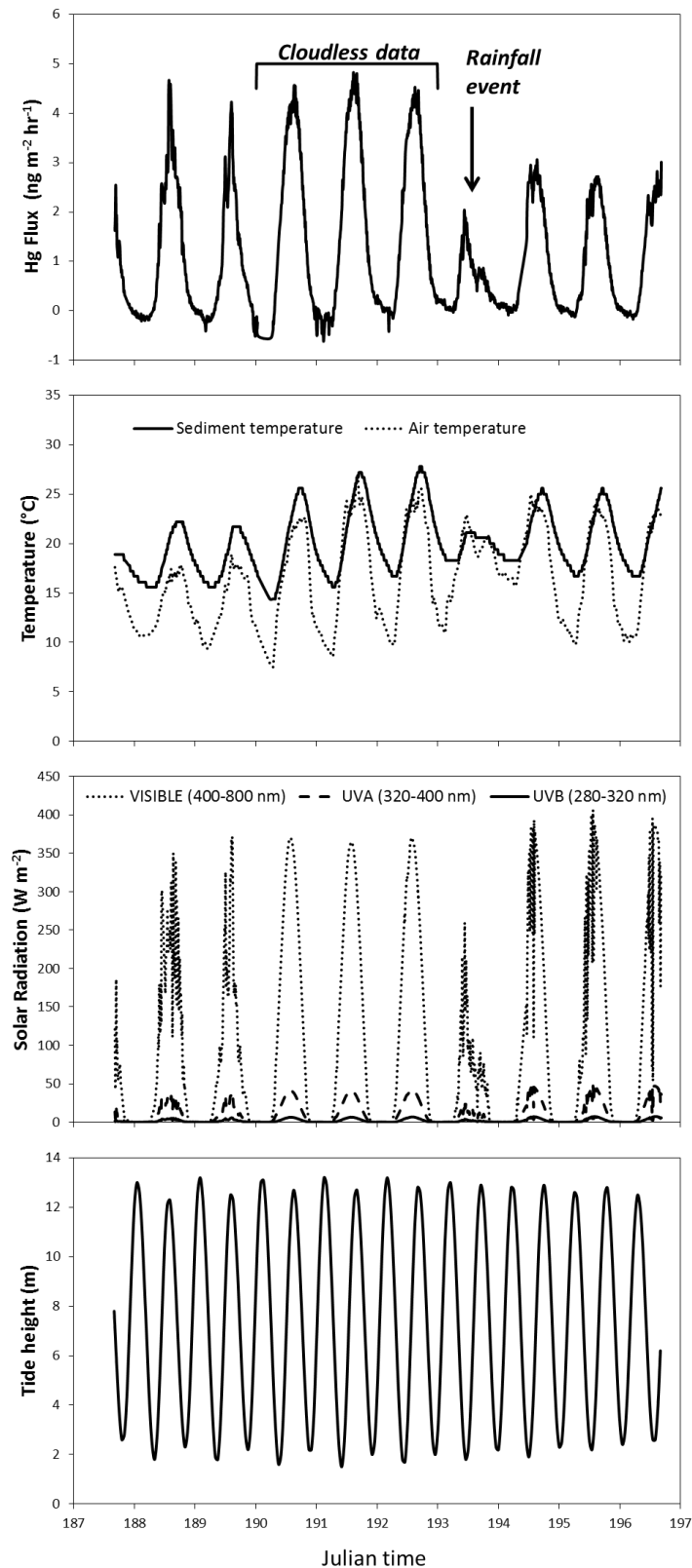
Figure 3 Time course data of gaseous Hg flux from the sediment, temperature of the sediment and the
ambient air, incoming solar radiation (in the visible, UVA and UVB spectrum), and tidal height
during the course of a continuous 9-day monitoring period from 6th to 15th July 2009 on a salt marsh
near Kingsport, Nova Scotia, in the Minas Basin of the Bay of Fundy. Three cloudless days (8th to
11th) and a 4 mm rainfall event (at 2pm on the 12th) are identified on the Hg flux plot.

188 During the course of the 9-day continuous monitoring of Hg flux from the salt marsh, there were three

189 cloudless days, from 8th to 11th July 2009 (Figure 3), which exposed the chamber to three diurnal

190 cycles of direct sunlight without interruption. There was also a 4mm rainfall event from 14:00 to

191 15:30 on 12th July (Figure 3) which suppressed the Hg flux thereafter. To aid our interpretation of the

192 data we analysed our dataset as four sub-datasets:

193 • All data (17:17 on 6th July to 15:27 on 15th July, n = 1212)

194 • Pre-rain data (17:17 on 6th July to 13:47 on 12th July, n = 789)

195 • Post rain data (13:57 on 12th July to 15:27 on 15th July, n = 422)

196 • Cloudless data (23:57 on 8th July to 23:57 on 11th July, n = 393)

197

198 <u>Hysteresis between solar radiation and Hg flux can be explained by sediment temperature</u>

199 There was a clear diurnal fluctuation in Hg flux, which peaked during the middle of the day at the

200 same time as the peak in solar radiation and air temperature (Figure 3). We found a positive

201 relationship between solar radiation (280-800 nm) and Hg flux (Figure 4), in agreement with several

202 other authors finding positive correlations at sites on grassland soils (Obrist et al., 2005), forest soils

203 (Choi and Holsen, 2009), oceans (Fantozzi et al., 2007), freshwater lakes (O'Driscoll et al., 2003),

204 snow (Mann et al., 2015), and salt marshes (Lee et al., 2000; Smith and Reinfelder, 2009). These

205 observations support the hypothesis that Hg flux is driven by photochemical reduction of Hg(II) to

206 Hg(0) and subsequent volatilisation of Hg(0) from the sediment. Because the intensity of solar

207 radiation at each waveband (UVA, UVB and visible) co-correlated, we could not elucidate which

208 wavelength was primarily responsible for stimulating the photochemical reactions.

209
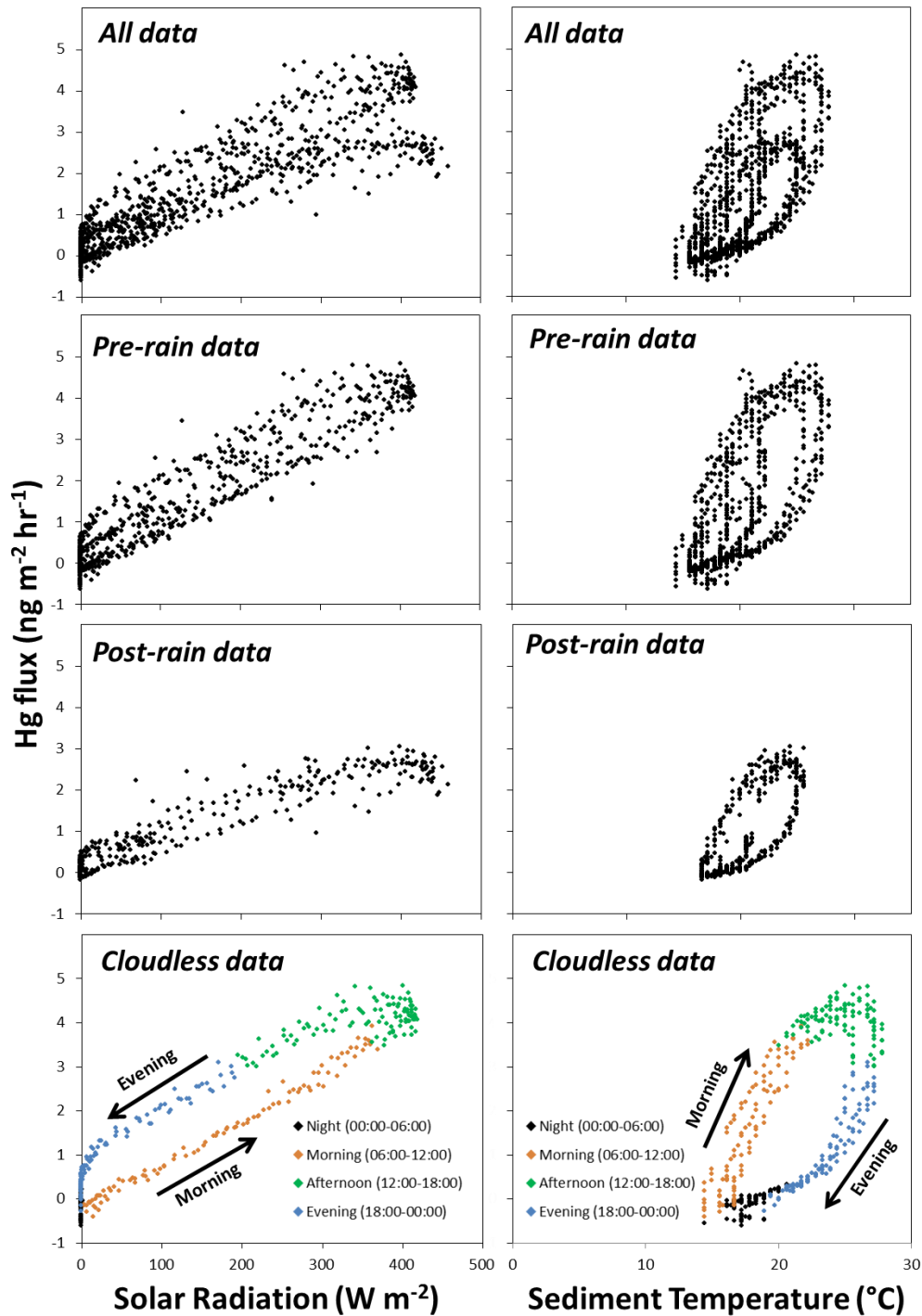
Figure 4 Gaseous Hg flux data from a salt marsh over a 9-day period plotted against the total incoming solar radiation in the range 280-800 nm and the temperature of the underlying sediment at a depth of 4 cm. All the data (from 6th to 15th July 2009) is presented in the top plot above the data collected before and after a 4 mm rainfall event (at 2pm on the 12th) are presented separately. Data collected during three cloudless days (8th to 11th) before the rainfall event is presented at the bottom and divided into measurements made during the night (00:00-06:00), morning (06:00-12:00), afternoon (12:00-18:00), and evening (18:00-00:00). There is a clear hysteresis in the data (observed most clearly in the cloudless dataset) as Hg flux is greater during the evening when the sediment is warm than in the morning when sediment is cool.

219   We found a clear cyclical diel relationship between solar radiation and Hg flux (Figure 4) which can

220   most easily be identified when plotting the data collected during three cloudless days from 8th to 11th

221   July 2009. At the same irradiance intensity, Hg flux is greater in the evening (18:00-00:00) than the

222   morning (06:00-12:00.) A similar relationship was found in morning and afternoon Hg flux

223   measurements made from coastal seawater (Lanzillotta and Ferrara, 2001). This cyclical relationship,

224   also referred to as hysteresis, can result from a time-lag between a controlling variable and its

225   measured effect, such as the delayed response of soil respiration to increasing temperature (Phillips et

226   al., 2011). However, it can also be a result of the simultaneous influence of several confounding

227   variables, such as solar radiation and temperature.

228

229   Several authors have observed positive correlations between Hg flux and air or soil temperature as

230   well as solar radiation (Lee et al., 2000; Lindberg et al., 1999; Obrist et al., 2005), and some note a

231   closer relationship between temperature and Hg flux than between solar radiation and Hg flux (Gillis

232   and Miller, 2000; Ma et al., 2013). However, these measurements confound one another since an

233   increase in incipient radiation causes an increase in temperature. In our study we did not find a

234   satisfactory correlation between Hg flux and either solar radiation, air temperature or sediment

235   temperature singularly since all three relationships result in a cyclical relationship (hysteresis) that is

236   most easily observed in the dataset collected on the cloudless days (Figure SI-1). Multiple linear

237   regression models fit using only solar radiation and sediment temperature as the explanatory variables

238   demonstrate that these two variables together can predict Hg flux in our sub-datasets with a high

239   degree of certainty (Figure 5). The models significantly (p<0.001) predict Hg flux using the pre-rain

240   dataset ($R^2 = 0.97$), the post-rain dataset ($R^2 = 0.95$) and the cloudless dataset ($R^2 = 0.99$). When

241   measurements at the same irradiance intensity are considered, Hg flux is greater in the evening

242   (18:00-00:00) when the salt marsh is warmer than in the morning (06:00-12:00) when the marsh is

243   cooler (Figure 4). The cyclical relationship between solar radiation and Hg flux can therefore be

244   explained by differences in the temperature of the sediment in the morning compared to the evening,

245   supported by Zhu et al (2015b) who observe Hg flux peaking in in concert with soil temperature.

246
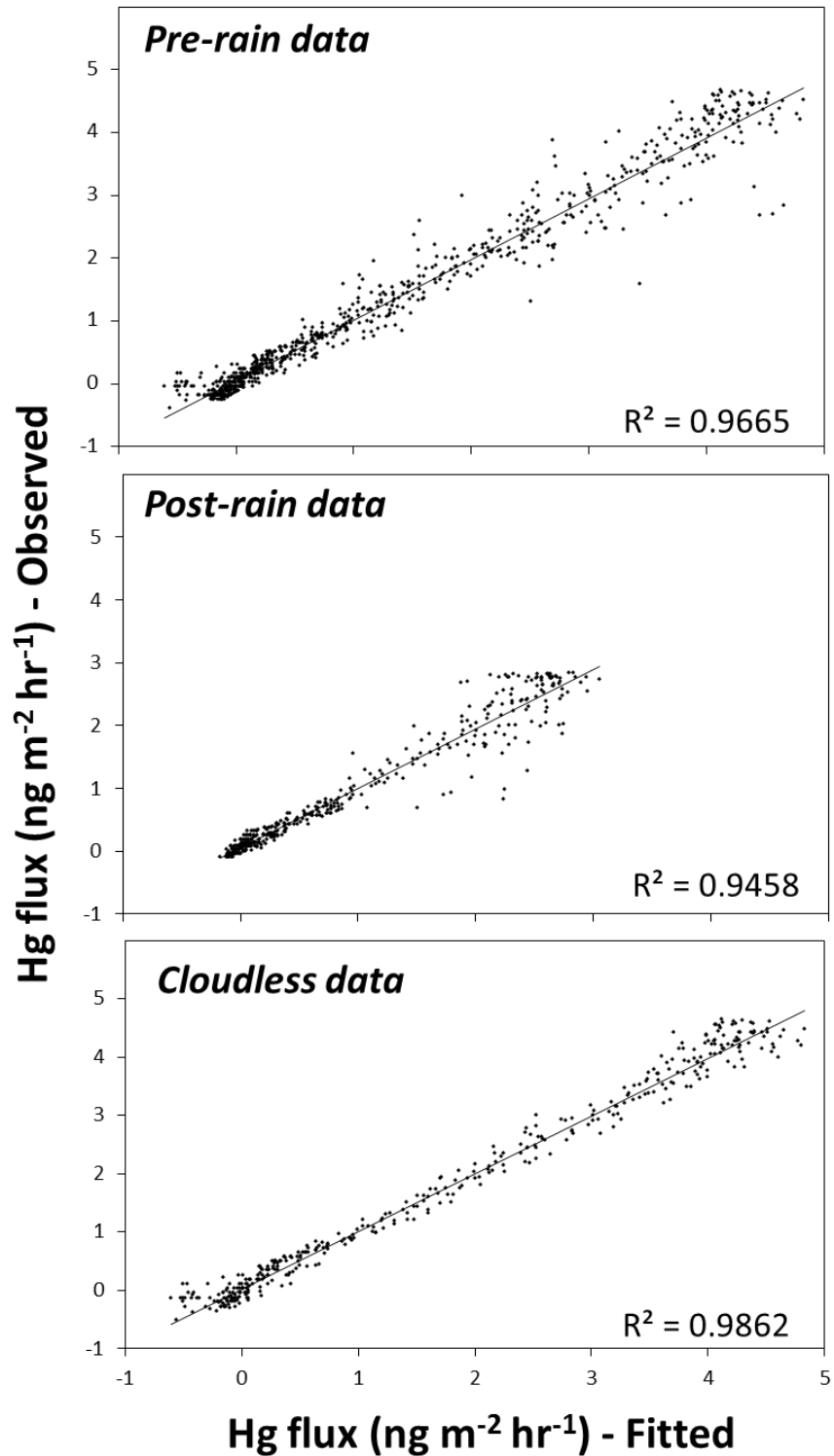
Figure 5 Gaseous Hg flux from a salt marsh before a 4 mm rainfall event (6th to 12th July 2009), after the rainfall event (12th to 15th), and during three cloudless days (8th to 11th) before the rainfall event plotted against fitted fluxes predicted using multiple linear regression models created with the same data. The models use solar radiation (280-800nm) and sediment temperature below the flux chamber and as explanatory variables.

252

253   There is uncertainty in the literature concerning whether temperature affects Hg flux by indirectly

254   increasing the proportion of Hg(II) that is available for photoreduction or whether it directly affects

255   Hg flux by providing energy for Hg(0) volatilization from soils (Bahlmann et al., 2006; Moore and

256   Carpi, 2005). Based on our observations, we advance the hypothesis that sediment temperature has an

257   indirect effect on Hg flux by directly influencing the rate of Hg(II) photoreduction, but not directly

258   influencing volatilization which may be due to abiotic desorption (Moore and Carpi, 2005), or the

259   result of transpiration by the salt marsh vegetation (Lindberg et al., 2002). Our hysteresis graphs show

260   that the direction of the cyclical relationship between sediment temperature and Hg flux occurs in the

261   opposite direction to the relationship between solar radiation and Hg flux (Figure 4). When

262   measurements at the same temperature are considered, Hg flux is greater in the morning (06:00-

263   12:00), when the solar radiation is higher, than the evening (18:00-12:00) when the solar radiation is

264   lower. If temperature has a direct effect on Hg flux by providing energy for desorption of Hg(0) from

265   sediment surfaces and subsequent volatilization from the soil then we would expect to see a weak

266   relationship between solar radiation and Hg flux in the evening because build-up of Hg(0) during the

267   day would continue to be emitted from the relatively warm sediment during the evening. Instead, it

268   seems that both solar radiation and sediment temperature are influencing the same rate-limiting

269   process responsible for Hg flux.

270

271   <u>Rainfall supresses Hg flux from salt marshes</u>

272   We observed lower Hg flux after a 4 mm 90 minute rainfall event on 12th July 2009 but an otherwise

273   similar cyclical relationship between solar radiation and Hg emissions (Figure 4) that can be

274   explained by the sediment being cool in the morning and warm in the evening (Figure 5). Our

275   observations contrast with several papers describing an immediate pulse of Hg released after rainfall

276   events due to a moisture-dependent displacement of Hg(0)-containing air from pores followed by a

277   greater rate of Hg flux from bare soil (Song and Van Heyst, 2005), desert soils (Lindberg et al., 1999),

278   agricultural soils (Briggs and Gustin, 2013), and floodplain soils (Wallschläger et al., 2000).

279   A key difference between the salt marsh where we made our observations and the soils monitored in

280   the abovementioned studies is that the salt marsh is tidally influenced. We hypothesised that the

281   incoming tide would cause displacement of Hg(0)-containing air from the sediment and provide a

282   clear influence of the tidal cycle on Hg flux. However, as observed by Smith and Reinfelder (2009)

283   and Lee et al (2000), we found no relationship between the tidal cycle and Hg flux. The rainfall event

284   occurred during an incoming tide and also did not result in a pulse of Hg flux. Therefore,

285   displacement of Hg(0)-containing air from sediment does not seem to contribute to Hg flux in salt

286   marshes, probably because the frequent movement of air in the salt marsh sediment (due to the tidal

287   cycle) does not allow Hg(0)-containing air to build up in the pores.

288   Rinklebe et al., (2010) demonstrate a negative correlation between soil water content and Hg flux in a

289   seasonally flooded terrestrial wetland, since the soils are generally wetter during the winter when

290   temperature and solar radiation are lower. However, in laboratory incubations, at constant

291   temperature, they reveal greater flux from wet or saturated soils compared to dry soils 24 and 48

292   hours after artificial wetting. These observations are further supported by data from Pannu et al.,

293   (2014) indicating that Hg flux from soils increases with increasing water-filled pore space (WFPS)

294   and peaked at 60% WFPS. However, this study also showed that increasing moisture to 80% WFPS

295   the Hg flux was considerably suppressed. Briggs and Gustin (2013) also note that after the initial

296   pulse following a rainfall event, the Hg flux can become supressed if the soil is saturated with water.

297   This suppression is due to a slower diffusivity of Hg(0) through water-filled pores as opposed to

298   through air-filled pores. In our experiment it is possible that some of the pores in the sediment became

299   saturated after the rainfall event and that slower diffusivity of Hg(0) is the reason for the suppressed

300   Hg flux. If transpiration of Hg(0) by wetland vegetation is a major mechanism controlling Hg flux

301   from the sediment (Lindberg et al., 2002) then the observed decrease in Hg flux may have been due to

302   stomatal closure and a subsequent decrease in the rate of transpiration under saturated conditions

303   (Pezeshki and DeLaune, 2012; Pezeshki, 2001).

304

<u>Environmental significance</u>

We provide here 9 days of continuous Hg flux measurements made on a salt marsh using the Dynamic Flux Chamber technique. Because the Hg flux measurements made can be directly related to the sediment underneath the chamber we elucidate an important diurnal mechanism that has not been previously identified. Our data supports the hypothesis that photoreduction of Hg(II) to Hg(0) is mediated by both sediment temperature and solar radiation and that photoreduction (rather than volatilisation of Hg(0)) is the rate limiting step in these sediments. This mechanistic insight reduces the uncertainty concerning the role of solar radiation and temperature in Hg flux from terrestrial surfaces. We also present data to suggest that the impact of rainfall on Hg flux behaves differently at coastal sites compared to terrestrial wetlands or soils. Here we show that Hg flux is suppressed after a rainfall event, possibly due to lower transpiration by salt marsh vegetation. The measurements of Hg flux and insights into the mechanisms controlling Hg flux presented here increase our knowledge of the global mercury cycle and provide a mechanistic framework for integrating coastal wetlands into global Hg flux models. However, caution should be exercised when applying this data for modelling since Hg flux is highly variable both spatially and temporally (During et al., 2009).

324 **References**

325 Agnan, Y., Le Dantec, T., Moore, C.W., Edwards, G.C., Obrist, D., 2016. New Constraints on
326 Terrestrial Surface–Atmosphere Fluxes of Gaseous Elemental Mercury Using a Global Database.
327 Environmental Science & Technology 50, 507-524. 10.1021/acs.est.5b04013

328 Bahlmann, E., Ebinghaus, R., Ruck, W., 2006. Development and application of a laboratory flux
329 measurement system (LFMS) for the investigation of the kinetics of mercury emissions from soils.
330 Journal of Environmental Management 81, 114-125. 10.1016/j.jenvman.2005.09.022

331 Briggs, C., Gustin, M.S., 2013. Building upon the Conceptual Model for Soil Mercury Flux: Evidence
332 of a Link Between Moisture Evaporation and Hg Evasion. Water, Air, & Soil Pollution 224, 1-13.
333 10.1007/s11270-013-1744-5

334 Canário, J., Caetano, M., Vale, C., Cesário, R., 2007. Evidence for Elevated Production of
335 Methylmercury in Salt Marshes. Environmental Science & Technology 41, 7376-7382.
336 10.1021/es071078j

337 Canário, J., Vale, C., Poissant, L., Nogueira, M., Pilote, M., Branco, V., 2010. Mercury in sediments
338 and vegetation in a moderately contaminated salt marsh (Tagus Estuary, Portugal). Journal of
339 Environmental Sciences 22, 1151-1157. 10.1016/S1001-0742(09)60231-X

340 Carpi, A., Lindberg, S.E., 1997. Sunlight-mediated emission of elemental mercury from soil amended
341 with municipal sewage sludge. Environmental Science & Technology 31, 2085-2091.
342 10.1021/es960910+

343 Choi, H.-D., Holsen, T.M., 2009. Gaseous mercury fluxes from the forest floor of the Adirondacks.
344 Environmental Pollution 157, 592-600. 10.1016/j.envpol.2008.08.020

345 Corbitt, E.S., Jacob, D.J., Holmes, C.D., Streets, D.G., Sunderland, E.M., 2011. Global source–
346 receptor relationships for mercury deposition under present-day and 2050 emissions scenarios.
347 Environmental Science & Technology 45, 10477-10484. 10.1021/es202496y

348 Desplanque, C., Mossman, D.J., 2001. Bay of Fundy tides. Geoscience Canada 28

349 During, A., Rinklebe, J., Böhme, F., Wennrich, R., Stärk, H.-J., Mothes, S., Du Laing, G., Schulz, E.,
350 Neue, H.-U., 2009. Mercury volatilization from three floodplain soils at the Central Elbe River,
351 Germany. Soil and Sediment Contamination 18, 429-444. 10.1080/15320380902962395

352 Fantozzi, L., Ferrara, R., Frontini, F.P., Dini, F., 2007. Factors influencing the daily behaviour of
353 dissolved gaseous mercury concentration in the Mediterranean Sea. Marine Chemistry 107, 4-12.
354 10.1016/j.marchem.2007.02.008

355 Gillis, A.A., Miller, D.R., 2000. Some local environmental effects on mercury emission and
356 absorption at a soil surface. Science of The Total Environment 260, 191-200. 10.1016/S0048-
357 9697(00)00563-5

358 Gregory Shriver, W., Evers, D.C., Hodgman, T.P., MacCulloch, B.J., Taylor, R.J., 2006. Mercury in
359 sharp-tailed sparrows breeding in coastal wetlands. Environmental Bioindicators 1, 129-135.
360 10.1080/15555270600695734

361   Hung, G.A., Chmura, G.L., 2006. Mercury accumulation in surface sediments of salt marshes of the
362   Bay of Fundy. Environmental Pollution 142, 418-431. 10.1016/j.envpol.2005.10.044

363   Krabbenhoft, D.P., Sunderland, E.M., 2013. Global change and mercury. Science 341, 1457-1458.
364   10.1126/science.1242838

365   Lanzillotta, E., Ferrara, R., 2001. Daily trend of dissolved gaseous mercury concentration in coastal
366   seawater of the Mediterranean basin. Chemosphere 45, 935-940. 10.1016/S0045-6535(01)00021-2

367   Lee, X., Benoit, G., Hu, X., 2000. Total gaseous mercury concentration and flux over a coastal
368   saltmarsh vegetation in Connecticut, USA. Atmospheric Environment 34, 4205-4213. 10.1016/S1352-
369   2310(99)00487-2

370   Lindberg, S., Zhang, H., Gustin, M., Vette, A., Marsik, F., Owens, J., Casimir, A., Ebinghaus, R.,
371   Edwards, G., Fitzgerald, C., 1999. Increases in mercury emissions from desert soils in response to
372   rainfall and irrigation. Journal of Geophysical Research: Atmospheres 104, 21879-21888.
373   10.1029/1999JD900202

374   Lindberg, S.E., Dong, W., Chanton, J., Qualls, R.G., Meyers, T., 2005. A mechanism for bimodal
375   emission of gaseous mercury from aquatic macrophytes. Atmospheric Environment 39, 1289-1301.
376   10.1016/j.atmosenv.2004.11.006

377   Lindberg, S.E., Dong, W., Meyers, T., 2002. Transpiration of gaseous elemental mercury through
378   vegetation in a subtropical wetland in Florida. Atmospheric Environment 36, 5207-5219.
379   10.1016/S1352-2310(02)00586-1

380   Ma, M., Wang, D., Sun, R., Shen, Y., Huang, L., 2013. Gaseous mercury emissions from subtropical
381   forested and open field soils in a national nature reserve, southwest China. Atmospheric Environment
382   64, 116-123. 10.1016/j.atmosenv.2012.09.038

383   Mann, E.A., Mallory, M.L., Ziegler, S.E., Avery, T.S., Tordon, R., O'Driscoll, N.J., 2015.
384   Photoreducible Mercury Loss from Arctic Snow Is Influenced by Temperature and Snow Age.
385   Environmental Science & Technology 49, 12120-12126. 10.1021/acs.est.5b01589

386   Mitchell, C.P., Gilmour, C.C., 2008. Methylmercury production in a Chesapeake Bay salt marsh.
387   Journal of Geophysical Research: Biogeosciences 113. 10.1029/2008JG000765

388   Moore, C., Carpi, A., 2005. Mechanisms of the emission of mercury from soil: Role of UV radiation.
389   Journal of Geophysical Research: Atmospheres 110. 10.1029/2004JD005567

390   Morel, F.M., Kraepiel, A.M., Amyot, M., 1998. The chemical cycle and bioaccumulation of mercury.
391   Annual review of ecology and systematics, 543-566. www.jstor.org/stable/221718

392   O'Driscoll, N.J., Beauchamp, S., Siciliano, S.D., Rencz, A.N., Lean, D.R.S., 2003. Continuous
393   Analysis of Dissolved Gaseous Mercury (DGM) and Mercury Flux in Two Freshwater Lakes in
394   Kejimkujik Park, Nova Scotia: Evaluating Mercury Flux Models with Quantitative Data.
395   Environmental Science & Technology 37, 2226-2235. 10.1021/es025944y

396   O'Driscoll, N.J., Canário, J., Crowell, N., Webster, T., 2011. Mercury speciation and distribution in
397   coastal wetlands and tidal mudflats: relationships with sulphur speciation and organic carbon. Water,
398   Air, & Soil Pollution 220, 313-326. 10.1007/s11270-011-0756-2

399   Obrist, D., Gustin, M.S., Arnone Iii, J.A., Johnson, D.W., Schorran, D.E., Verburg, P.S.J., 2005.
400   Measurements of gaseous elemental mercury fluxes over intact tallgrass prairie monoliths during one
401   full year. Atmospheric Environment 39, 957-965. 10.1016/j.atmosenv.2004.09.081

402   Pannu, R., Siciliano, S.D., O'Driscoll, N.J., 2014. Quantifying the effects of soil temperature, moisture
403   and sterilization on elemental mercury formation in boreal soils. Environmental Pollution 193, 138-
404   146. 10.1016/j.envpol.2014.06.023

405   Pezeshki, S., DeLaune, R., 2012. Soil oxidation-reduction in wetlands and its impact on plant
406   functioning. Biology 1, 196-221. 10.3390/biology1020196

407   Pezeshki, S.R., 2001. Wetland plant responses to soil flooding. Environmental and Experimental
408   Botany 46, 299-312. 10.1016/S0098-8472(01)00107-1

409   Phillips, C.L., Nickerson, N., Risk, D., Bond, B.J., 2011. Interpreting diel hysteresis between soil
410   respiration and temperature. Global Change Biology 17, 515-527. 10.1111/j.1365-2486.2010.02250.x

411   Rinklebe, J., During, A., Overesch, M., Du Laing, G., Wennrich, R., Stärk, H.-J., Mothes, S., 2010.
412   Dynamics of mercury fluxes and their controlling factors in large Hg-polluted floodplain areas.
413   Environmental Pollution 158, 308-318. 10.1016/j.envpol.2009.07.001

414   Sizmur, T., Canário, J., Gerwing, T.G., Mallory, M.L., O'Driscoll, N.J., 2013. Mercury and
415   methylmercury bioaccumulation by polychaete worms is governed by both feeding ecology and
416   mercury bioavailability in coastal mudflats. Environmental Pollution 176, 18-25.
417   10.1016/j.envpol.2013.01.008

418   Sizmur, T., Godfrey, A., O'Driscoll, N.J., 2016. Effects of coastal managed retreat on mercury
419   biogeochemistry. Environmental Pollution 209, 99-106. 10.1016/j.envpol.2015.11.016

420   Smith, L.M., Reinfelder, J.R., 2009. Mercury volatilization from salt marsh sediments. Journal of
421   Geophysical Research: Biogeosciences 114. 10.1029/2009JG000979

422   Sommar, J., Zhu, W., Lin, C.-J., Feng, X., 2013. Field Approaches to Measure Hg Exchange Between
423   Natural Surfaces and the Atmosphere—A Review. Critical Reviews in Environmental Science and
424   Technology 43, 1657-1739. 10.1080/10643389.2012.671733

425   Song, X., Van Heyst, B., 2005. Volatilization of mercury from soils in response to simulated
426   precipitation. Atmospheric Environment 39, 7494-7505. 10.1016/j.atmosenv.2005.07.064

427   Steudler, P.A., Peterson, B.J., 1984. Contribution of gaseous sulphur from salt marshes to the global
428   sulphur cycle. Nature 311, 455-457. 10.1038/311455a0

429   UNEP, U., 2013. Global Mercury Assessment 2013: Sources, Emissions, Releases and Environmental
430   Transport. United Nations Environment Programme Chemicals Branch, Geneva, Switzerland.

431   Wallschläger, D., Herbert Kock, H., Schroeder, W.H., Lindberg, S.E., Ebinghaus, R., Wilken, R.-D.,
432   2000. Mechanism and significance of mercury volatilization from contaminated floodplains of the
433   German river Elbe. Atmospheric Environment 34, 3745-3755. 10.1016/S1352-2310(00)00083-2

434   Zhang, Y., Jacob, D.J., Horowitz, H.M., Chen, L., Amos, H.M., Krabbenhoft, D.P., Slemr, F., St.
435   Louis, V.L., Sunderland, E.M., 2016. Observed decrease in atmospheric mercury explained by global

436   decline in anthropogenic emissions. Proceedings of the National Academy of Sciences 113, 526-531.
437   10.1073/pnas.1516312113

438   Zhu, W., Sommar, J., Lin, C.J., Feng, X., 2015a. Mercury vapor air–surface exchange measured by
439   collocated micrometeorological and enclosure methods – Part II: Bias and uncertainty analysis.
440   Atmos. Chem. Phys. 15, 5359-5376. 10.5194/acp-15-5359-2015

441   Zhu, W., Sommar, J., Lin, C.J., Feng, X., 2015b. Mercury vapor air–surface exchange measured by
442   collocated micrometeorological and enclosure methods – Part I: Data comparability and
443   method characteristics. Atmos. Chem. Phys. 15, 685-702. 10.5194/acp-15-685-2015

444

445